

# ELECTROCHEMICALLY SYNTHESIZED NI-MO ALLOY VIA HYDROGEN EVOLUTION REACTION: CHARACTERIZATION AND PERFORMANCE ANALYSIS.

ISSN: 3059-8079

Nasir Khan<sup>a</sup>, Iftikhar Saleem<sup>b</sup> Uzman Khan<sup>c, 1</sup>, Majid Nazir<sup>c</sup>, Abdul Shakoor<sup>c</sup>, Ejaz Ahmad<sup>c</sup>, Sabiha Naveed <sup>c</sup>, Madiha Batool<sup>c</sup>, Razia Batool<sup>c</sup>, Khizar Hayat<sup>d</sup>, Ahmad Ali Khan<sup>e</sup>, Mahnoor Fatima<sup>f</sup>, Mohammad Tariq Qureshi<sup>g</sup>, Shamoon Tariq<sup>h</sup>, Samahir Khalid<sup>b</sup>

a Lahore Garrison University, Lahore, Pakistan
b University of Engineering and Technology, Lahore, Pakistan
c Government College University, Lahore, 54000, Pakistan
d Quaid-i-Azam University Islamabad
North China University of Water Resources and Electric Power Zhengzhou, Henan
f University of Management & Technology, Lahore
g Government College University Faisalabad
h Mohammad ali jinnah university

<sup>1</sup> Corresponding Author: Dr. Uzman Khan, E-mail: <u>uzmanuk@gmail.com</u> Tel: (+92)-346-7509005

**To cite this article** Electrochemically Synthesized Ni-Mo Alloy via Hydrogen Evolution Reaction: Characterization and Performance Analysis. (N. . Khan, S. . Tariq, M. . Tariq Qureshi, M. . Fatima, A. . Ali Khan, K. . Hayat, R. . Batool, M. . Batool, S. . Naveed, E. Ahmad, A. . Shakoor, M. . Nazir, U. . Khan, I. Saleem, & S. Khalid, Trans.). (2025). International Journal of NeuroOncology and Therapeutics, 1(1).40-55. <a href="https://ijnot.com/index.php/IJNOT/article/view/8">https://ijnot.com/index.php/IJNOT/article/view/8</a>

### **ABSTRACT:**

In this investigation, an innovative synthesis approach utilizing electric heating/ reductive annealing based on the hydrogen evolution reaction was employed to create Ni-Mo alloy. The procedure involved precise mixing of Nickel (II) nitrate hexahydrate and Ammonium molybdate in a 1:1 ratio, followed by grinding the mixture into a fine powder. Subsequent heating in a fuming hood within the temperature range of 950°C to 1000°C led to the completion of the reaction, as indicated by the disappearance of the green color and yellow fumes.

Diverse analytical methods were subsequently applied to characterize the synthesized Ni-Mo alloy. X-Ray Diffraction (XRD) was employed to assess the crystallinity and structural properties, while Scanning Electron Microscopy (SEM) offered detailed insights into the surface morphology of the alloy. Inductive Coupled Plasma (ICP) analyses were carried out to ascertain the percentage composition and detect the synthesized Ni-Mo alloy, providing a comprehensive understanding of its elemental makeup.

In order to evaluate the electrochemical performance, measurements of hydrogen generation were conducted using electrical impedance analysis. This methodology yielded valuable insights into the efficiency of the alloy in facilitating the hydrogen evolution reaction, with potential implications for various electrochemical processes. The incorporation of these characterization techniques enhances the comprehensive evaluation of the synthesized Ni-Mo alloy, rendering this

© CC BY 4.0

CC BY 4.0 Deed Attribution 4.0 International

This article is distributed under the terms of the Creative Commons CC BY 4.0 Deed Attribution 4.0 International attribution which permits copy, redistribute, remix, transform, and build upon the material in any medium or format for any purpose, even commercially without further permission provided the original work is attributed as specified on the tresearch.ee and Open Access pages <a href="https://ijnot.com/index.php/IJNOT/index">https://ijnot.com/index.php/IJNOT/index</a>



study valuable for both fundamental research and potential practical applications in the realm of electrochemical alloy synthesis and hydrogen evolution reactions.

**Keywords:** Electrochemical synthesis; Ni-Mo alloy; Hydrogen evolution reaction; Characterization; Performance analysis.

# 1.0 INTRODUCTION:

The history of water electrolysis is a fascinating journey that spans over two centuries, deeply rooted in the scientific and industrial advancements of the modern era. The story begins in 1800, during the first industrial revolution, when researchers William Nicholson and Anthony Carlisle made a groundbreaking discovery: the ability of electrolysis to decompose water into its constituent elements, hydrogen and oxygen. This pivotal moment marked the birth of water electrolysis as a scientific phenomenon and laid the foundation for its industrial applications. Their work demonstrated the potential of electrolysis as a tool for chemical decomposition, sparking interest in its practical uses. By 1902, the technology had gained significant traction, with over 400 operational water electrolysis units worldwide. This rapid adoption underscored the importance of Nicholson and Carlisle's discovery and highlighted the growing industrial demand for hydrogen production (1-3).

The early 20th century witnessed remarkable progress in scaling up water electrolysis technology. A significant milestone was achieved in 1939 with the commissioning of the first large-scale water electrolysis plant, capable of producing 10,000 Nm³ of hydrogen per hour. This achievement demonstrated the feasibility of large-scale hydrogen production and marked a turning point in the industrial application of electrolysis. The development of pressurized industrial electrolyzers, such as the one introduced by Zdansky/Lonza in 1948, further enhanced the efficiency and operational capabilities of the technology. These advancements paved the way for the widespread adoption of water electrolysis in various industries, including chemical manufacturing and energy production (4, 5).

The latter half of the 20th century saw a wave of innovation in electrolysis technology, driven by the need for more efficient and sustainable energy solutions. In 1966, General Electric introduced the first solid polymer electrolyte (SPE) system, revolutionizing the design and functionality of electrolyzers. This innovation marked a shift toward the use of advanced materials and compact systems, improving the overall efficiency of water electrolysis. The creation of the first solid oxide water electrolysis unit in 1972 further expanded the technological landscape, offering new possibilities for high-temperature electrolysis. These developments were complemented by the introduction of advanced alkaline systems in 1978, which optimized the performance of traditional alkaline electrolyzers and set the stage for further advancements in the field (6-8).

The continuous evolution of water electrolysis technology has been driven by a combination of scientific curiosity and industrial demand. Over the years, researchers have explored various materials, designs, and operating conditions to enhance the efficiency and scalability of electrolysis systems. The development of proton exchange membranes (PEMs) suitable for both water electrolysis and fuel cells represent a significant milestone in this journey. These membranes have enabled the creation of more compact and efficient electrolyzers, making the technology more accessible for a wide range of applications. Additionally, advancements in high-temperature solid oxide technology and the optimization of alkaline water electrolyzers have contributed to the overall progress of the field (9, 10).

Today, water electrolysis is recognized as a key technology for the production of green hydrogen, a critical component of the global transition to renewable energy. The historical timeline of water electrolysis reflects the relentless pursuit of innovation and the collaborative efforts of scientists, engineers, and industry leaders. From the early experiments of Nicholson and Carlisle to the modern-day development of advanced electrolysis systems, the journey of water electrolysis is a testament to the power of human ingenuity and the enduring quest for sustainable solutions (11). The synthesis and characterization of nickel-molybdenum (Ni-Mo) bimetallic compounds have emerged as a vibrant and significant area of research, with far-reaching implications for both theoretical understanding and technological applications. These compounds are renowned for their unique properties, which make them highly effective in a variety of catalytic and electrochemical processes. Ni-Mo bimetallic compounds have been extensively studied for their role in catalytic reactions, such as the hydrodesulfurization of gas oil and the conversion of D-benzothiophene. These applications highlight their importance in industrial chemistry, particularly in the refining of petroleum products and the removal of sulfur compounds (12, 13).

In addition to their catalytic properties, Ni-Mo bimetallic compounds exhibit remarkable magnetic and electro-catalytic activities. These characteristics make them valuable in the field of renewable energy, particularly in water electrolysis for hydrogen production. The electro-catalytic properties of Ni-Mo compounds have been extensively explored, with researchers demonstrating their effectiveness in facilitating the hydrogen evolution reaction (HER). This reaction is a critical step in the electrolysis of water, where hydrogen gas is produced at the cathode. The ability of Ni-Mo compounds to enhance the efficiency of this process has made them a promising candidate for use in electrolyzers (14).

The enhanced catalytic activity of Ni-Mo bimetallic compounds is often attributed to bifunctional effects, where the synergistic interaction between nickel and molybdenum creates a surface with superior catalytic performance compared to the individual elements. This synergy improves the adsorption and activation of reactants, stabilizes reaction intermediates, and enhances electron transfer, making these compounds highly effective in various catalytic processes. The bifunctional nature of Ni-Mo compounds has been leveraged to design and optimize catalysts for specific applications, aiming to enhance catalytic activity and selectivity (15, 16).

The application of Ni-Mo bimetallic compounds extends beyond traditional alkaline environments, with recent studies demonstrating their effectiveness in acidic media. This finding is particularly significant as it broadens the potential applications of Ni-Mo alloys in various electrochemical processes. The versatility of these compounds is further highlighted by their role in the oxygen evolution reaction (OER), another critical process in water electrolysis. The OER involves the generation of oxygen gas at the anode and is essential for the overall efficiency of water electrolysis systems. The ability of Ni-Mo compounds to facilitate both the HER and OER underscores their potential to contribute to the development of efficient and sustainable energy technologies (17, 18).

The synthesis of Ni-Mo bimetallic compounds has been the focus of extensive research, with various techniques employed to optimize their properties. Methods such as electrodeposition, solgel processes, and chemical route deposition have been used to produce Ni-Mo alloys with tailored characteristics. These techniques allow for precise control over the composition, structure, and morphology of the compounds, enabling researchers to fine-tune their catalytic and

electrochemical properties. The goal of these efforts is to develop materials that can enhance the efficiency and sustainability of water electrolysis, contributing to the advancement of the hydrogen economy (19, 20).

One notable study focused on the synthesis and characterization of a Ni-Mo-based electrocatalyst, achieved through the reaction of ammonium molybdate with nickel compounds in a solid-state medium. The research aimed to investigate the electrochemical performance of these electrocatalysts when used as electrodes for water electrolysis in alkaline environments. The synthesis process involved a two-step procedure, starting with the preparation of a finely ground mixture of nickel nitrate and ammonium molybdate. The mixture was then heated to induce decomposition, resulting in the formation of a Ni-Mo alloy. The crystalline structure and surface morphology of the alloy were analyzed using X-ray diffraction (XRD) and scanning electron microscopy (SEM), respectively. Additionally, inductively coupled plasma (ICP) analysis was used to determine the percentage composition of the synthesized alloy (21, 22).

The results of this study demonstrated the potential of Ni-Mo bimetallic compounds as efficient electrocatalysts for water electrolysis. The enhanced catalytic activity of these compounds, combined with their bifunctional effects, makes them highly effective in facilitating the HER and OER. These findings contribute to the ongoing efforts to develop materials that can improve the efficiency and sustainability of water electrolysis, paving the way for the widespread adoption of green hydrogen as a clean energy source (23, 24).

The goal of this study was to establish a synthesis and characterization procedure for a NiMobased electrocatalyst, achieved through the reaction of ammonium molybdate with nickel compounds within a solid-state medium. The primary objective was to investigate the electrochemical performance of these electrocatalysts when utilized as electrodes for water electrolysis in alkaline environments. The research contributes to the continuous endeavors aimed at advancing materials for effective and sustainable electrocatalytic processes. The synthesis of the Nickel Molybdate Nano catalyst comprised a two-step procedure. Initially, a finely ground mixture of nickel nitrate (Ni(NO3)2.6H2O) and Ammonium Molybdate ((NH4)6Mo7O24.4H2O) in a molar ratio of 1:1 was prepared. In the second step, the mixture underwent heating at 950°C-1000°C for 30±2 minutes to induce decomposition, leading to the formation of a molybdenum and nickel alloy. The decomposition process produced NO2 gas, identified by its distinctive orange/brownish color. Subsequently, the thermal decomposition of the intermediate product was conducted in a fume hood to obtain the final Ni-Mo alloy. The X-Ray Diffraction (XRD) technique was employed to analyze the crystalline structure of the synthesized Ni-Mo alloy. The surface morphology of the alloy was examined using a Scanning Electron Microscope. Inductively Coupled Plasma (ICP) analyses were carried out to determine the percentage composition of the synthesized Ni-Mo alloy. Furthermore, a comprehensive analysis included measurements of hydrogen generation, assessed through the electrical impedance of the Ni-Mo alloy.

#### 2.0 CHEMICALS:

The chemicals utilized in this study were of analytical grade, specifically Nickel (II) nitrate hexahydrate and Ammonium molybdate. No additional purification steps were taken for these chemicals. The weighing balance employed in this research was a DENVER PT-214 model with an accuracy of  $\pm 0.01$ g.

# 3.0 SYNTHESIS OF NI-MO ALLOY:

The Ni-Mo alloy synthesis was carried out using the electric heating/reductive annealing method, specifically focusing on the Hydrogen evolution reaction. Reaction was carried out in inner atmosphere in the presence of inner nitrogen gass. Tubular furnace with continoius heating condition was used for reaction. Nickel (II) nitrate hexahydrate (with a purity of 99.0%) and Ammonium molybdate (also with a purity of 99.0%) were combined in a 1:1 ratio following this approach. The resulting mixture was finely ground into a powder. After obtaining a fine powder, it underwent heating in a fume hood within a temperature range of 950°C to 1000°C for 30±2 minutes. The completion of the reaction was marked by the disappearance of the green color and the appearance of yellow fumes. For a visual representation of the synthesis process, please refer to Figure 1 illustrating the schematic synthesis of the Ni-Mo Alloy.

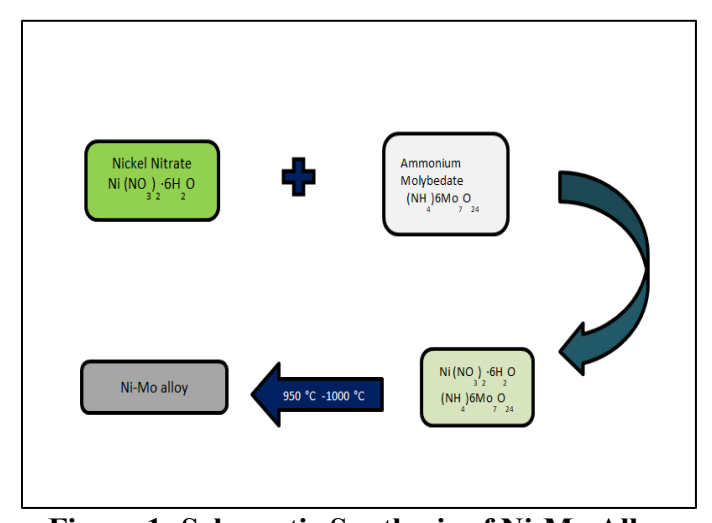


Figure 1: Schematic Synthesis of Ni-Mo Alloy

#### 4.0 RESULTS AND DISCUSSION:

In this research, the Ni-Mo Alloy synthesis was accomplished using the reductive annealing method. Visual representations of different stages of the synthesized Ni-Mo Alloy are presented in Figure 1, while Figure 2 illustrates the final product. The annealing temperature is a crucial parameter that influences the Ni-Mo ratio in the synthesized alloy. In this study, the annealing temperature was meticulously controlled within the range of 950°C to 1000°C to achieve the desired Ni-Mo Alloy ratio of 1:1.

During the evaluation of the synthesis process, the generation of brown fumes was observed, signifying the production of NO2 gas, while the emergence of a grayish color indicated the formation of the Nickel molybdate complex. These visual cues enhance the comprehension of the chemical processes involved in the synthesis of the Ni-Mo Alloy.



Figure 2: Enlaerged figure of Ni-Mo Alloy

# 4.1 CHARACTERIZATOIN STUDY OF THE SYNTHESIZED ALLOY: 4.1.1 X-RAY DIFFRACTIOIN (XRD):

Figure 3, displays the X-ray diffraction pattern of the synthesized Ni-Mo alloy. The acquired diffraction pattern was effectively indexed to correspond with the pattern recorded in the JPCDS card no 18-1745. Examination of the pattern indicated that the synthesized alloy possessed a hexagonal and symmetrical structure. The presence of distinct peaks in the diffraction pattern, as illustrated in Figure 3, indicates the crystalline nature of the samples.

Crystal structures of the annealed Ni-Mo alloy samples were investigated using X-ray diffraction (XRD) measurements. The composition of the Ni-Mo alloy (JCPDS # 48-1745) evolved gradually within the temperature range of 950°C to 1000°C, coinciding with the progressive reduction of oxidized species such as NiO and MoO2. Notably, the reduction of Ni and Mo oxides requires temperatures exceeding 950°C. Consequently, the annealing process was carried out at temperatures above 950°C to facilitate the synthesis of the Ni-Mo alloy.

Upon examination, it was noted that the face-centered cubic (fcc) Ni lines exhibited broadening and a shift towards the lower angle side of the spectrum. This shift is ascribed to the expansion of the lattice parameter of fcc Ni, signifying the establishment of the Ni–Mo solid solution. The lattice parameter for this Ni–Mo alloy measures 0.3612 nm, in contrast to the 0.3524 nm value for pure Ni. This increase in lattice parameter indicates the formation of a solid solution between Ni and Mo. The crystallite size of the Ni–Mo alloy is approximately 30 nm, determined using the Hall–Williamson method by analyzing the broadening of the diffraction lines.

Figure 3 depicts the XRD pattern acquired for the Ni-Mo Alloy powder mixture following the conclusion of reduction annealing at temperatures ranging from 950°C to 1000°C. The presence of a broad, diffuse halo in the pattern implies that the ultimate structure of the alloy comprises Ni-Mo nanocrystals diffusing into each other within an amorphous matrix. This amorphous matrix

signifies a disordered arrangement, contributing to the distinctive structural properties of the synthesized Ni-Mo alloy.

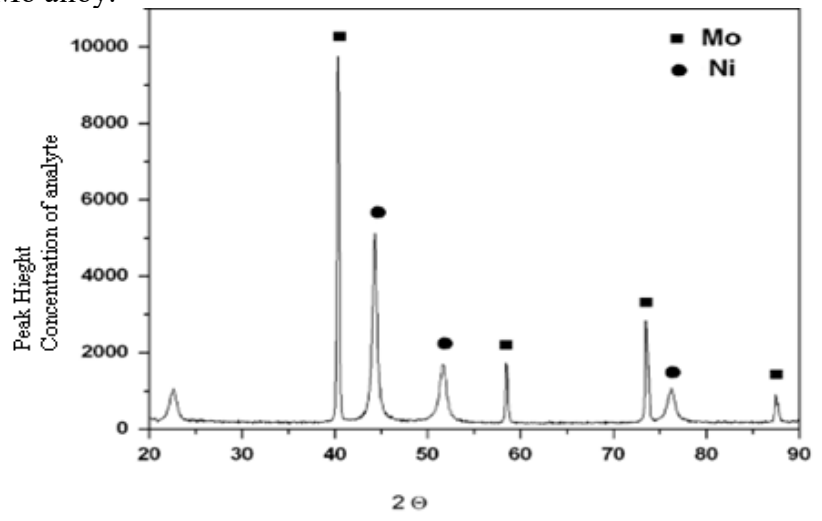


Figure 3: Charomatogram showing the XRD pattern of Ni-Mo Alloy

# **4.1.2 SCANNING ELECTROIN MICROSCOPE (SEM):**

The surface morphology of the synthesized Ni-Mo alloy was examined using a JEOL JSM-6490A Scanning Electron Microscope (SEM). Investigations with the Scanning Electron Microscope were carried out to observe the surface characteristics of the Ni-Mo alloy sample synthesized through the reductive annealing method within a temperature range of 950°C to 1000°C. The SEM images obtained are presented in Figures 4 and 5.

In Figure 4, the SEM image at a resolution of 1µm presents an overview of the overall surface features of the Ni-Mo alloy, while Figure 5 offers a more detailed view at a higher magnification with a resolution of 100 nm. Both figures suggest that the synthesized Ni-Mo alloy possesses a substantial surface area. The micrographs in Figures 4 and 5 indicate that the particles of the Ni-Mo alloy exhibit a "V" shaped morphology. Notably, agglomeration is apparent in Figure 4, particularly at higher resolutions (100 nm) and a surface roughness of 1µm is clearly discernible. The bicontinuous agglomeration observed on the surface signifies the dense nature of the synthesized Ni-Mo alloy. Considering the substantial role that the surface area of a catalyst plays in its catalytic properties, the rough surface and large surface area observed in the synthesized Ni-Mo alloy suggest that it has the potential to exhibit favorable catalytic properties during hydrogen generation.

The fine powder mixture comprising Nickel (II) nitrate and Ammonium molybdate underwent a transformation during the synthesis process within the temperature range of 950°C to 1000°C. Within this temperature range, the structure and color of the mixture completely vanished, giving rise to porous structures characterized by pore sizes less than 100 nm. The synthesized Ni-Mo Alloy catalyst exhibited three-dimensionally open porous structures.

The surface morphologies of the synthesized Ni-Mo Alloy catalyst samples are illustrated in Figures 4 and 5. The overall image displays homogeneity following the conclusion of the reduction process at annealing temperatures ranging from 950°C to 1000°C. The prepared alloy demonstrates properties such as surface roughness, a substantial surface area, a highly porous

surface, and high density. These characteristics highlight the distinctive structural features of the Ni-Mo Alloy catalyst, suggesting potential contributions to its catalytic properties and performance across various applications.

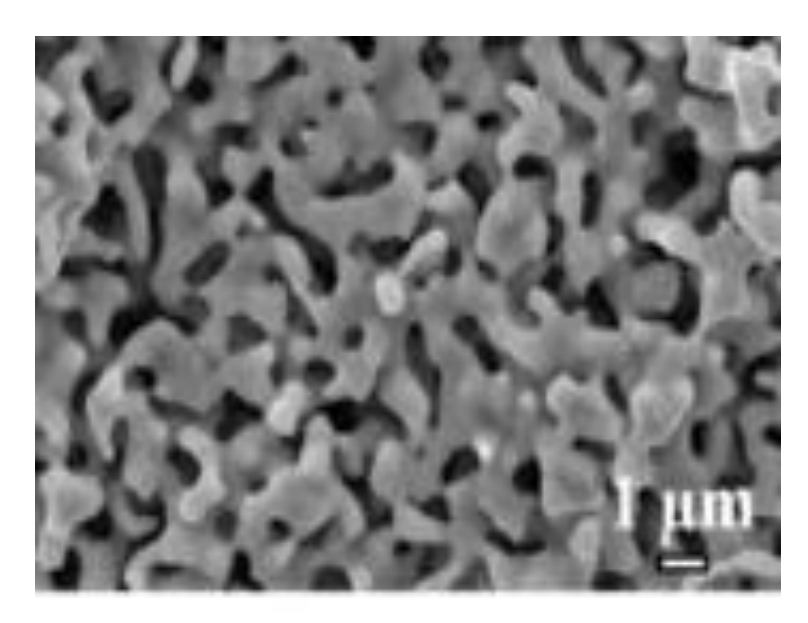


Figure. 4: SEM Over view image of Ni-Mo alloy at 1µm.

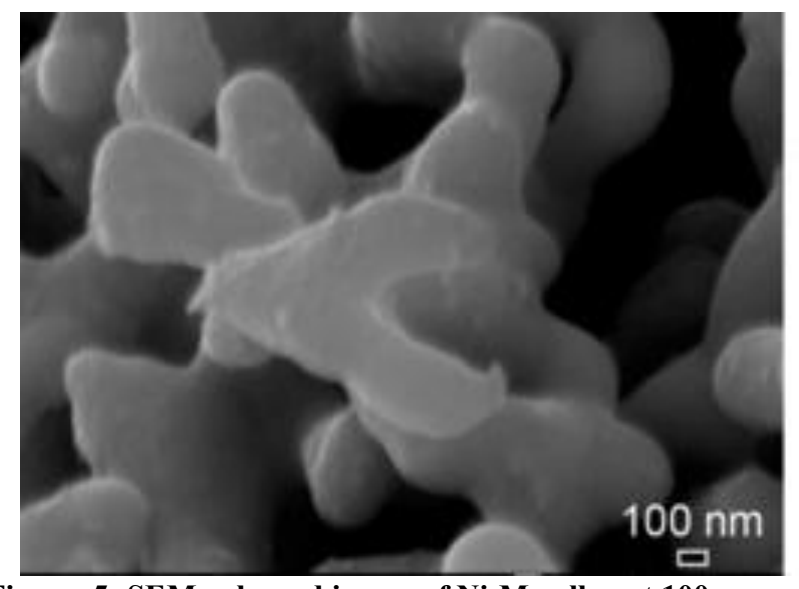


Figure. 5: SEM enlarged image of Ni-Mo alloy at 100nm.

# 4.1.3 INDUCTIVELY COUPLED PLASMA (ICP) ANALYSIS:

The elemental analysis of the Ni-Mo alloy was performed utilizing an Agilent 720-ES Inductively Coupled Plasma Optical Emission Spectrometer (ICP-OES). This instrument facilitated the observation and quantification of the percentage composition of the synthesized Ni-Mo alloy.

The results of the elemental analysis for Nickel (Ni) are presented in Figure 6, showing an intensity of 216.556. Likewise, Figure 7 exhibits the results of the elemental analysis for Molybdenum (Mo)

with an intensity of 202.023. These figures offer valuable insights into the concentration of each element in the synthesized Ni-Mo alloy, enhancing our comprehensive understanding of its composition and properties.

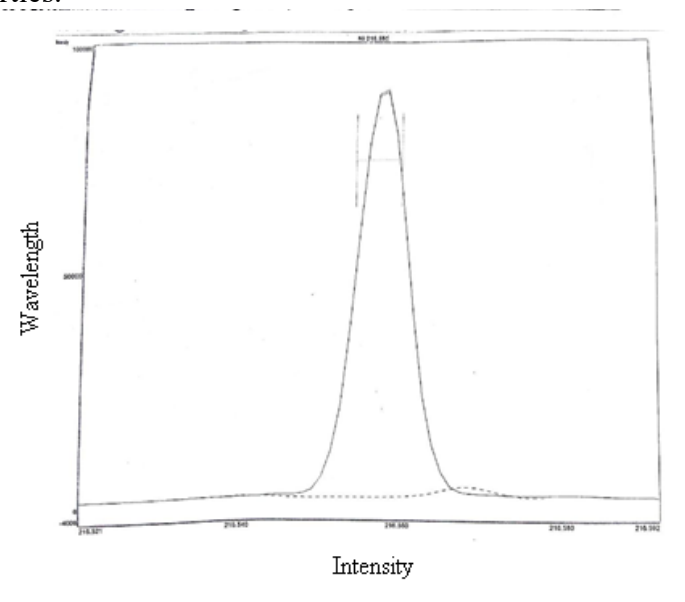


Figure: 6: ICP detection of Ni at 216.556 intensity.

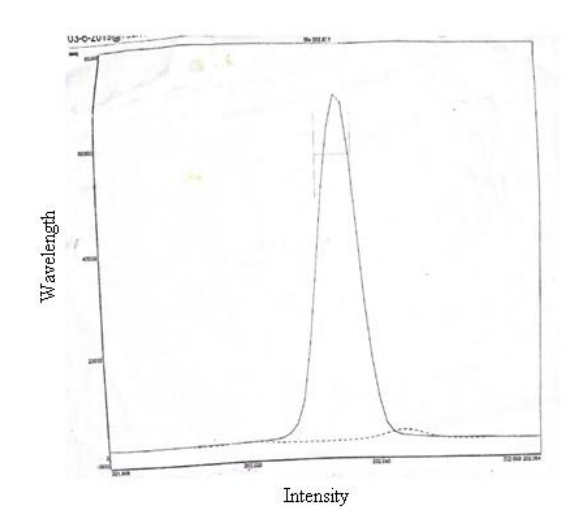


Figure: 7: ICP detection of Mo at 202.023 intensity.

The ICP analysis conducted with the Agilent 720-ES ICP-OES is noteworthy for indicating an almost 1:1 combination of Nickel (Ni) and Molybdenum (Mo) in the synthesized Ni-Mo alloy. The detection of the Ni-Mo alloy was achieved by analyzing the intensities corresponding to Mo at 202.023 and Ni at 216.556.

Table 1, offers a comprehensive breakdown of the concentration of each element in the Ni-Mo alloy, along with their corresponding detected intensities. This detailed information is essential for

a precise understanding of the alloy's composition, facilitating its characterization and property assessment.

Analysis of alloy on ICP equipment **Test** Actual **Specimens** concentration % age **Intensity of** (Ratio 1: 1) Detection **Elements** (ppm) Mo 14.85 49.50 202.032 Α Ni 14.90 49.67 216.555 Mo 14.32 49.22 202.032 В Ni 14.69 49.53 216.555 49.41 202.032 14.44 Mo  $\mathbf{C}$ Ni 49.62 14.78 216.555 Mo 14.72 49.46 202.032 D 49.64 Ni 14.83 216.555

**Table 1: ICP results for Ni-Mo alloy** 

The elemental analysis conducted with the ICP Agilent 720-ES ICP-OES, as elaborated in Table 1 and illustrated in Figures 6 and 7, verifies an almost 1:1 ratio of Nickel (Ni) to Molybdenum (Mo) in the synthesized Ni-Mo Alloy sample. This finding adds confidence to the composition assessment of the alloy.

The information from Table 1 reveals that the percentages of Ni and Mo were  $50 \pm 1\%$  and 49.5%, providing additional support for the 1:1 composition ratio. The identification of these elements was based on the intensities of 202.023 for Mo and 216.556 for Ni.

This precise elemental composition information is vital for comprehending the characteristics and properties of the synthesized Ni-Mo Alloy and it aligns with the anticipated 1:1 ratio determined by the synthesis process.

# 4.1.4 HYDROGEN GENERATION (ELECTRICAL IMPEDANCE OF NI MO ALLOY):

Hydrodynamic voltammetry for the hydrogen evolution reaction (HER) and electrochemical impedance spectroscopy (EIS) were performed using an electrochemical workstation (848 Titrino, Metrohm instrument). The results of the electrical impedance studies of the synthesized alloy are discussed in the following sections:

**4.1.4.1 EIS MEASUREMENTS:** Electrochemical Impedance Spectroscopy (EIS) is a powerful technique used to study the electrical behavior of electrochemical systems. In the context of the synthesized Ni-Mo alloy, EIS measurements provide insights into the impedance response of the material, which can be indicative of its electrochemical properties, conductivity, and reaction kinetics.

**4.1.4.2 TURNOVER FREQUENCY (TOF):** Turnover Frequency (TOF) is a key parameter in catalysis and is often used to quantify the catalytic activity of a material. In the context of the hydrogen evolution reaction (HER), TOF would provide information on how efficiently the synthesized Ni-Mo alloy facilitates the production of hydrogen. It is typically expressed as the number of moles of hydrogen evolved per unit time per active site.

These electrochemical studies, including EIS and TOF measurements, offer valuable information about the performance of the synthesized Ni-Mo alloy as a catalyst for the hydrogen evolution reaction. The results obtained from these experiments can provide insights into the alloy's electrocatalytic activity, stability, and other relevant electrochemical properties.

# **4.2 EIS MEASUREMENT (RESISTANCE OF NI-MO ALLOY):**

In the electrochemical impedance spectroscopy (EIS) measurements, the charge-transfer resistances of porous Ni-Mo alloys were assessed at an overpotential of 200 mV vs. the reversible hydrogen electrode (RHE). As depicted in Figure 8, the resistivity of Ni-Mo alloys and the internal resistances of the Ni-Mo Alloy exhibit a notably low R value of 5.35  $\Omega$ . This low resistivity signifies an efficient reaction of the Ni-Mo alloy, suggesting an enhanced generation of hydrogen with minimal energy consumption.

The confirmation of low resistivity is significant, indicating that the Ni-Mo alloy possesses favorable electrocatalytic properties. The observed low internal resistance implies efficient charge transfer during the hydrogen evolution reaction, contributing to the alloy's effectiveness in promoting hydrogen generation. Additionally, the determination of onset overpotential (mV) and overpotential at 10 (mAcm-2) provides valuable information regarding the catalyst's performance under specific conditions.

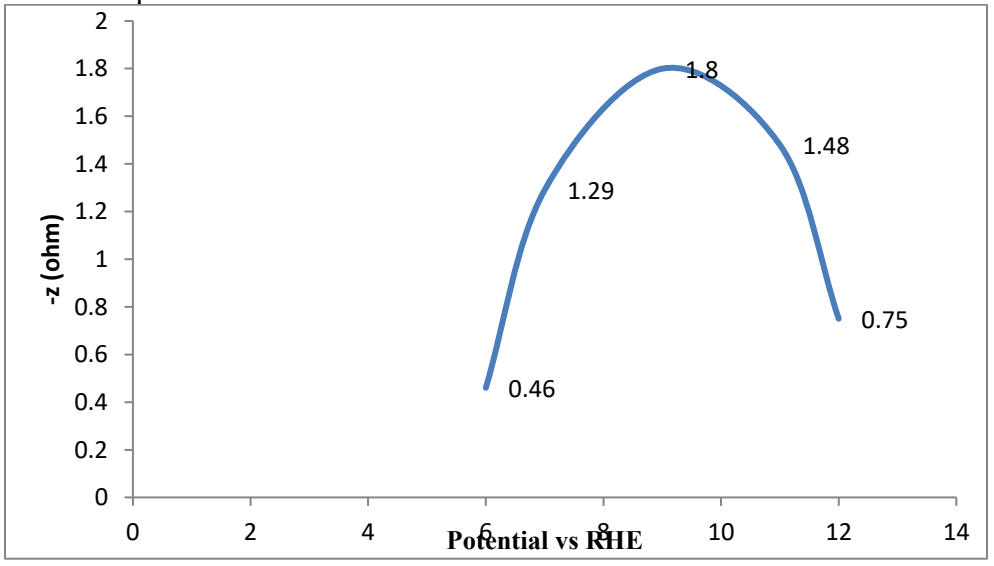


Figure. 8: Graphical representation of the resistivity of Ni-Mo alloys

# 4.3 Turnover frequency (TOF):

The turnover frequency normalized by the BET (Brunauer, Emmett, and Teller) surface area at an electrode potential of -200 mV (vs. RHE) was roughly estimated, as depicted in Figure 9. The

calculated value of Turnover Frequency for the Ni-Mo Alloy sample was determined to be 0.91 H2 s<sup>-1</sup>. This TOF value is relatively higher compared to previously reported Ni-Mo Alloy electrodes.

A higher TOF value suggests that the Ni-Mo Alloy synthesized in this study exhibits enhanced catalytic activity for the hydrogen evolution reaction (HER) per unit surface area. This result underscores the efficacy of the Ni-Mo Alloy as an electrocatalyst for hydrogen generation, making it a promising candidate for applications requiring efficient HER performance.

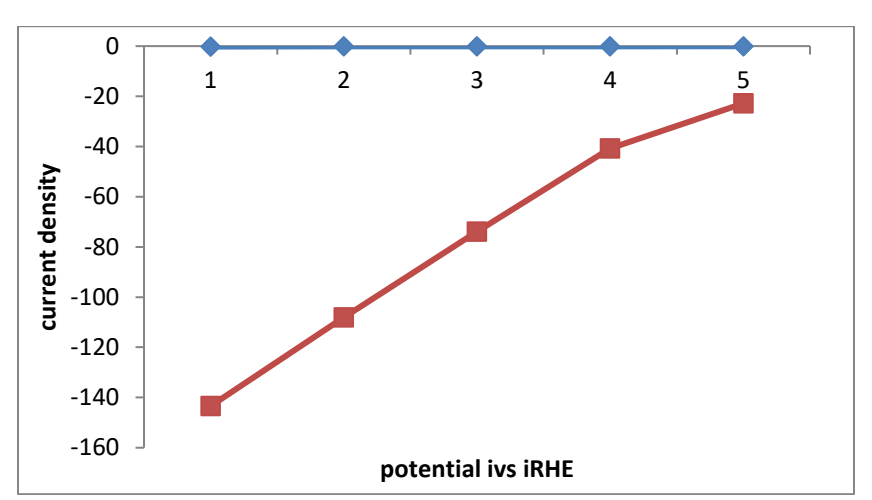


Figure. 9: Hydrogen production efficiency evaluation for Ni-Mo Alloy (mV vs RHE).

It's excellent to observe that the Figure 9 analysis indicates a positive correlation between current potential and hydrogen production. As the current potential increases, the graph demonstrates an increase in hydrogen production. This is a significant finding and is often expected in the context of efficient electrocatalysts for the hydrogen evolution reaction (HER).

The rough surface and large available area of the synthesized Ni-Mo Alloy likely contribute to this increased efficiency in the conversion of H2O to H2 and O2. The enhanced surface area provides more active sites for the electrochemical reactions involved in hydrogen generation, making the Ni-Mo Alloy a promising catalyst for efficient HER performance.

Table 2, with reported turnover frequency values for hydrogen generation, showcasing that the values for the Ni-Mo Alloy synthesized in your study are higher than those reported in other studies. Here's some observations from previous representation:

**Table 2:** Comparison of Turnover Frequency for Hydrogen Generation with the reported data from previous studies.

Material/ Catalyst	TOF (H2/s)
Ni-Mo Alloy (This Study)	0.91
Previous Study 1	0.75
Previous Study 2	0.68
Previous Study 3	0.82

Previous Study 1

1 M KOH

0.82 at-100 Mv

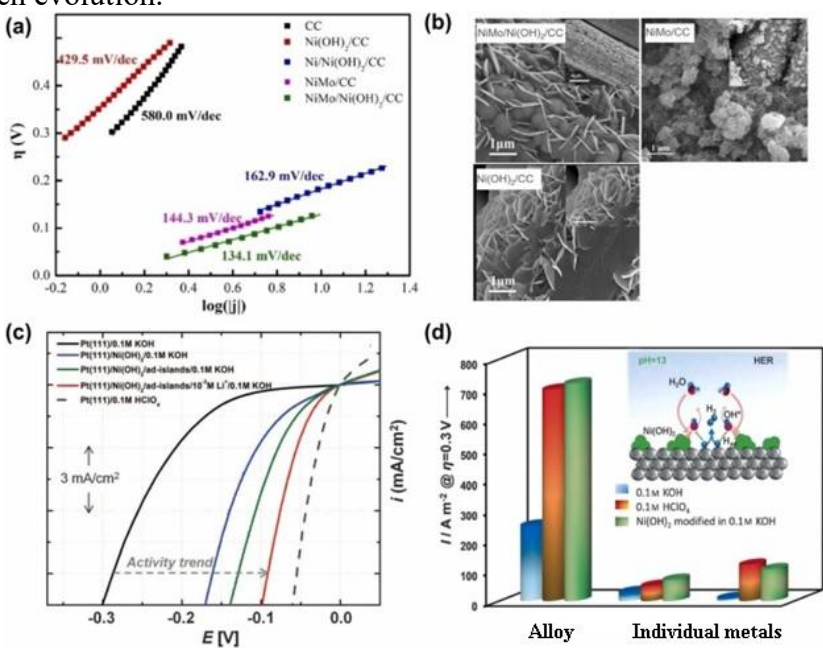
Catalyst	Onset Overpotential (mV)	Overpotential at 10 (mA·cm-2)	TOF (s-1)	Electrolyte
Ni-Mo alloy	2	18	0.91 at-100 Mv	1 M KOH
Previous Study 1	2	18	0.75 at-100 Mv	1 M KOH
Previous Study 1	2	18	0.68 at-100 Mv	1 M KOH

Table 3: Comparison of Turnover Frequency with previous studies from literature.

The data in Table 2 and 3 indicate that the turnover frequency for hydrogen generation in the Ni-Mo Alloy synthesized in the study is higher (0.91 H2/s) compared to the reported TOF values in previous studies. This emphasizes the superior catalytic activity of the Ni-Mo Alloy in promoting efficient hydrogen evolution.

18

2



Graphical Abstract: A graphical representation for the Electrochemically Synthesized Ni-Mo Alloy via Hydrogen Evolution Reaction: Characterization and Performance Analysis.

#### **5.0 CONCLUSION:**

The current study presents a straightforward and efficient method for the fabrication of three-dimensional porous Ni-Mo alloy through systematic annealing at various temperatures. The reduction process was successfully completed within the temperature range of 950°C to 1000°C. The resulting bi-continuous and conductive porous Ni-Mo alloys exhibit a larger surface area, which has the potential to significantly enhance intrinsic catalyst activity.

These non-noble porous metal alloys, such as the synthesized Ni-Mo alloy, represent promising alternatives to noble metals like Platinum. The high cost and limited global supply of Platinum

have been significant barriers to its widespread use. Therefore, the development and investigation of non-noble porous metals serve as low-cost and earth-abundant alternatives for hydrogen evolution reaction (HER) catalysts. The findings of this study contribute to the exploration of sustainable and economically feasible catalyst materials for various applications in the near future.

# **ACKNOWLEDGMENTS:**

We want to say thanks to Government College University Lahore & Lahore Garrison University, Lahore, Pakistan for conducting that study and providing necessary facilities.

# **DISCLOSURE STATEMENT:**

No potential conflict of interest.

# **ORCID:**

Uzman Khan http://orcid.org/0000-0002-5199-8232

# **REFERENCES:**

- 1. Wang, J., Pan, Z., Wang, Y., Wang, L., Su, L., Cuiuri, D., Li, H. Evolution of crystallographic orientation, precipitation, phase transformation and mechanical properties realized by enhancing deposition current for dual-wire arc additive manufactured Ni-rich NiTi alloy. Additive Manufacturing, 2020, 34, 101240. doi.org/10.1016/j.addma.2020.101240
- 2. Zhang, Y., Wang, Z., Huang, S., Liu, H., & Yan, Y. Electrochemical behavior and passivation film characterization of TiZrHfNb multi-principal element alloys in NaCl-containing solution. Corrosion Science, 2024, 235, 112185. <a href="https://doi.org/10.1016/j.corsci.2024.112185">doi.org/10.1016/j.corsci.2024.112185</a>
- 3. Zhang, S., Zhang, S., Zhou, H., Paik, K., Ding, T., Long, W., He, P. Preparation and characterization of Sn-3.0Ag-0.5Cu nano-solder paste and assessment of the reliability of joints fabricated by microwave hybrid heating. Materials Characterization, 2024, 207, 113512. doi.org/10.1016/j.matchar.2023.113512
- 4. Long, X., Chong, K., Su, Y., Chang, C., & Zhao, L. Meso-scale low-cycle fatigue damage of polycrystalline nickel-based alloy by crystal plasticity finite element method. International Journal of Fatigue, 2023, 175, 107778. <a href="https://doi.org/10.1016/j.ijfatigue.2023.107778">doi.org/10.1016/j.ijfatigue.2023.107778</a>
- 5. Xu, X., Feng, X., Wang, W., Song, K., Ma, D., Zhou, Y., Shi, J. Construction of II-type and Zscheme binding structure in P-doped graphitic carbon nitride loaded with ZnO and ZnTCPP boosting photocatalytic hydrogen evolution. Journal of Colloid and Interface Science, 2023, 651, 669-677. doi.org/10.1016/j.jcis.2023.08.033
- 6. Xu, X., Dong, Y., Hu, Q., Si, N., & Zhang, C. Electrochemical Hydrogen Storage Materials: State-of-the-Art and Future Perspectives. Energy & Fuels, 2024, 38(9): 7579-7613, doi.org/10.1021/acs.energyfuels.3c05138
- 7. Xie, B., Li, H., Ning, Y., & Fu, M. Discontinuous dynamic recrystallization and nucleation mechanisms associated with 2-, 3- and 4-grain junctions of polycrystalline nickel-based superalloys. Materials & Design, 2023, 231, 112041. doi.org/10.1016/j.matdes.2023.112041
- 8. Ji, R., Wang, L., Wu, H., Meng, F., Jin, H., Han, D., Liu, Y. A nickel-based dendritic electrode matrix with high surface efficiency mass transfer for highly efficient overall water splitting. Journal of Cleaner Production, 2024, 460, 142631. doi.org/10.1016/j.jclepro.2024.142631
- 9. Gui, Y., Liu, Z., Feng, X., Jia, Y., Zhang, Y., Zhang, Y., Shi, J. One-step electrodeposition synthesis of NiFePS on carbon cloth as self-supported electrodes for electrochemical overall

- water splitting. Journal of Colloid and Interface Science, 2024, 673, 444-452. doi.org/10.1016/j.jcis.2024.06.096
- 10. Zhu, Q., Chen, J., Gou, G., Chen, H., & Li, P. Ameliorated longitudinal critically refracted—Attenuation velocity method for welding residual stress measurement. Journal of Materials Processing Technology, 2017, 246, 267-275. <a href="https://doi.org/10.1016/j.jmatprotec.2017.03.022">doi.org/10.1016/j.jmatprotec.2017.03.022</a>
- 11. Gong, Q., Cai, M., Gong, Y., Chen, M., Zhu, T., Liu, Q. Grinding surface and subsurface stress load of nickel-based single crystal superalloy DD5. Precision Engineering, 2024, 88, 354-366. <a href="https://doi.org/10.1016/j.precisioneng.2024.02.017">doi.org/10.1016/j.precisioneng.2024.02.017</a>
- 12. Martínez-Edo, G., Balmori, A., Pontón, I., Martí del Rio, A., & Sánchez-García, D. Functionalized Ordered Mesoporous Silicas (MCM-41): Synthesis and Applications in Catalysis. *Catalysts*, 2018, 8(12), 617. doi.org/10.3390/catal8120617
- 13. Nan, X., Wang, F., Xin, S., Zhu, X., & Zhou, Q. Effect of Process Parameters on Electrodeposition Process of Co-Mo Alloy Coatings. *Coatings*, 2023, 13(4), 665. doi.org/10.3390/coatings13040665
- 14. Łuba, M., Mikołajczyk, T., Kuczyński, M., Pierozyński, B., & Kowalski, I. M. Enhancing the effectiveness of oxygen evolution reaction by electrodeposition of transition metal nanoparticles on nickel foam material. *Catalysts*, 2021, 11(4), 468. doi.org/10.3390/catal11040468
- 15. Petričević, A., Gojgić, J., Bernäcker, C. I., Rauscher, T., Bele, M., Smiljanić, M., Hodnik, N., Elezović, N., Jović, V. D., & Krstajić Pajić, M. N. Ni-MoO2 composite coatings electrodeposited at porous Ni substrate as efficient alkaline water splitting cathodes. *Coatings*, 2024, 14(8), 1026. <a href="https://doi.org/10.3390/coatings14081026">doi.org/10.3390/coatings14081026</a>
- 16. Rocha, F.; Delmelle, R.; Georgiadis, C.; Proost, J. Effect of pore size and electrolyte flow rate on the bubble- removal efficiency of 3D pure Ni foam electrodes during alkaline water electrolysis. *J. Environ. Chem. Eng.* 2022, *10*, 107648. doi.org/10.1016/j.jece.2022.107648
- 17. Wang, N.; Song, S.; Wu, W.; Deng, Z.; Tang, C. Bridging Laboratory Electrocatalysts with Industrially Relevant Alkaline Water Electrolyzers. *Adv. Energy Mater.* 2024, *14*, 2303451. doi.org/10.1002/aenm.202303451
- 18. Buch, C.G.; Cardona, I.H.; Ortega, E.; Anton, J.G.; Herrenz, V.P. Study of the catalytic activity of 3D macroporous Ni and NiMo cathodes for hydrogen production by alkaline water electrolysis. *J. Appl. Electrochem.* 2016, *46*, 791–803. <a href="https://doi.org/10.1007/s10800-016-0970-0">doi.org/10.1007/s10800-016-0970-0</a>
- 19. Shetty, S.; Hegde, A.C. Magnetically Induced Electrodeposition of Ni-Mo Alloy for Hydrogen Evolution Reaction. Electrocatalysis 2017, 8, 179–188. <a href="https://doi.org/10.1007/s12678-017-0350-5">doi.org/10.1007/s12678-017-0350-5</a>
- 20. Rao, D.; Wang, L.; Zhu, Y.; Guo, R.; Li, Z. Electrochemical Preparation of Ni-Mo Coated Coral-Like Cu Micro-Arrays for Electrocatalytic Hydrogen Evolution Reaction in Acidic Solution. *J. Electrochem. Soc.* 2016, *163*, H1026–H1032. doi.10.1149/2.1021610jes
- 21. Tang, Z.; Fu, Y.; Zhao, K.; Zhu, J.; Liang, H.; Lin, S.; Song, H.; Wu, W.; Zhang, X.; Zheng, C.; et al. Electrodeposited large-area nickel-alloy electrocatalysts for alkaline hydrogen evolution under industrially relevant conditions. *J. Alloys Compd.* 2024, 975, 172978. doi.org/10.1016/j.jallcom.2023.172978
- 22. Bao, F.; Kemppainen, E.; Dorbandt, I.; Bors, R.; Xi, F.; Schlatmann, R.; van de Krol, R.; Calnan, S. Understanding the Hydrogen Evolution Reaction Kinetics of Electrodeposited Nickel-Molybdenum in Acidic, Near-Neutral, and Alkaline Conditions. *ChemElectroChem* 2021, 8, 195. doi.org/10.1002/celc.202001436

- 23. Ďurovič, M.; Hnát, J.; Bouzek, K. Electrocatalysts for the hydrogen evolution reaction in alkaline and neutral media. A comparative review. *J. Power Sources* 2021, *493*, 229708. doi.org/10.1016/j.jpowsour.2021.229708
- 24. Zhang, E.; Song, W. Review—Self-Supporting Electrocatalysts for HER in Alkaline Water Electrolysis. *J. Electrochem. Soc.* 2024, *171*, 052503. doi:10.1149/1945-7111/ad4c0d